YMTHE, Volume *30*

Supplemental Information

Targeting HLA-DR loss in hematologic malignancies with an inhibitory chimeric antigen receptor

Fan Fei, Liang Rong, Nan Jiang, Alan S. Wayne, and Jianming Xie

Supplemental Figures

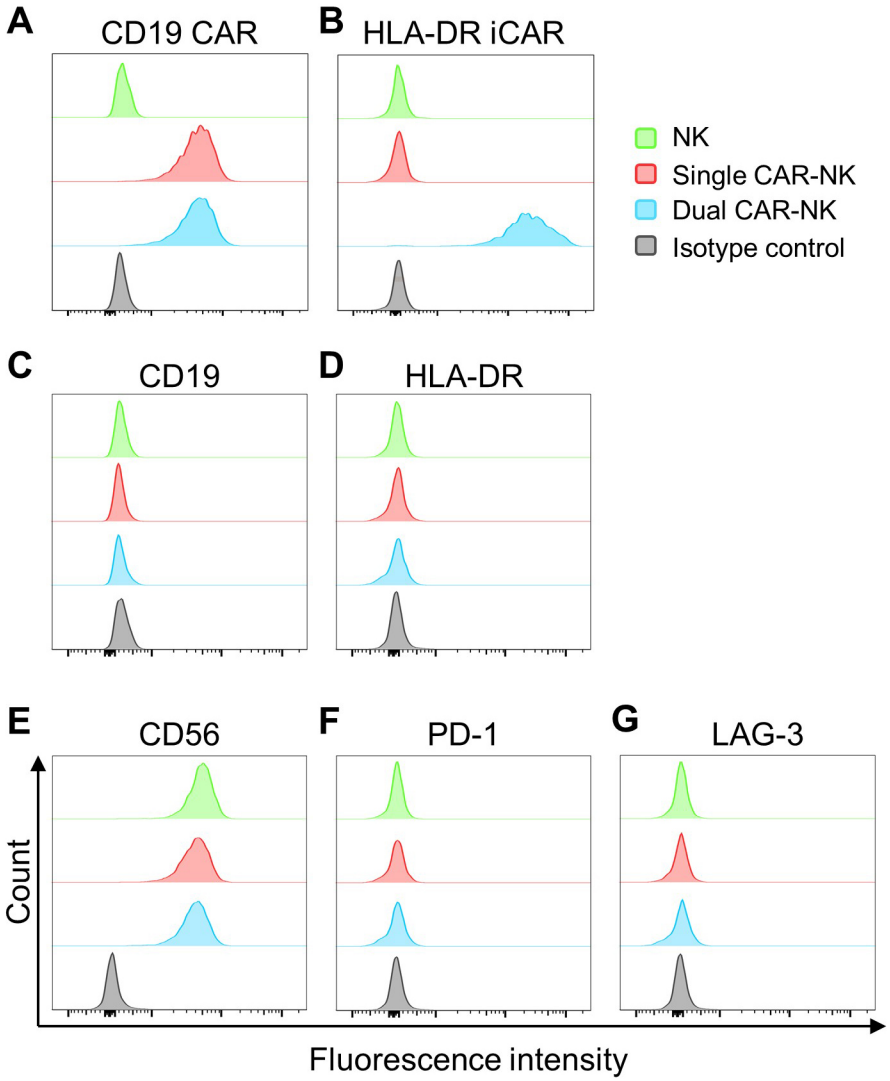

Figure S1. Flow cytometric analysis of NK, single CAR-NK, and dual CAR-NK cells. Cells were stained for CD19 CAR (**A**), HLA-DR iCAR (**B**), CD19 (**C**), HLA-DR (**D**), CD56 (**E**), PD-1 (**F**), and LAG-3 (**G**). Negative controls were NK cells stained with isotype control antibodies.

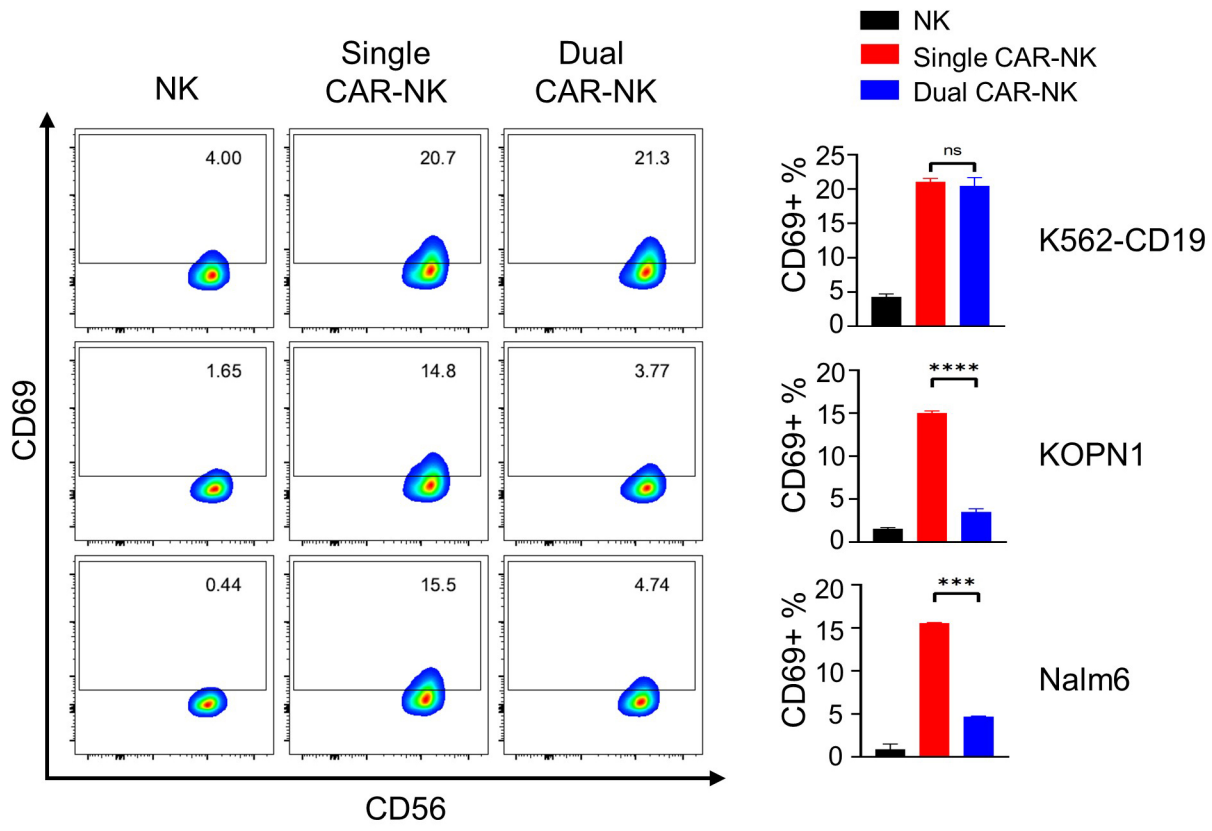

Figure S2. Flow cytometric analysis of CD69 expression on NK and CAR-NK cells. NK, single CAR-NK, and dual CAR-NK cells were cocultured with K562-CD19, KOPN1, or Nalm6 cells for 4 hours at 37ºC. Cells were stained with a PE-Cy7-labeled anti-CD69 antibody and an APC-labeled anti-CD56 antibody followed by flow cytometric analysis. Data are shown as mean ± SEM of two independent experiments. Statistical significance is calculated by unpaired two-tailed Student's t-test. **** $p<0.0001$; *** $p<0.001$; ns: not significant.

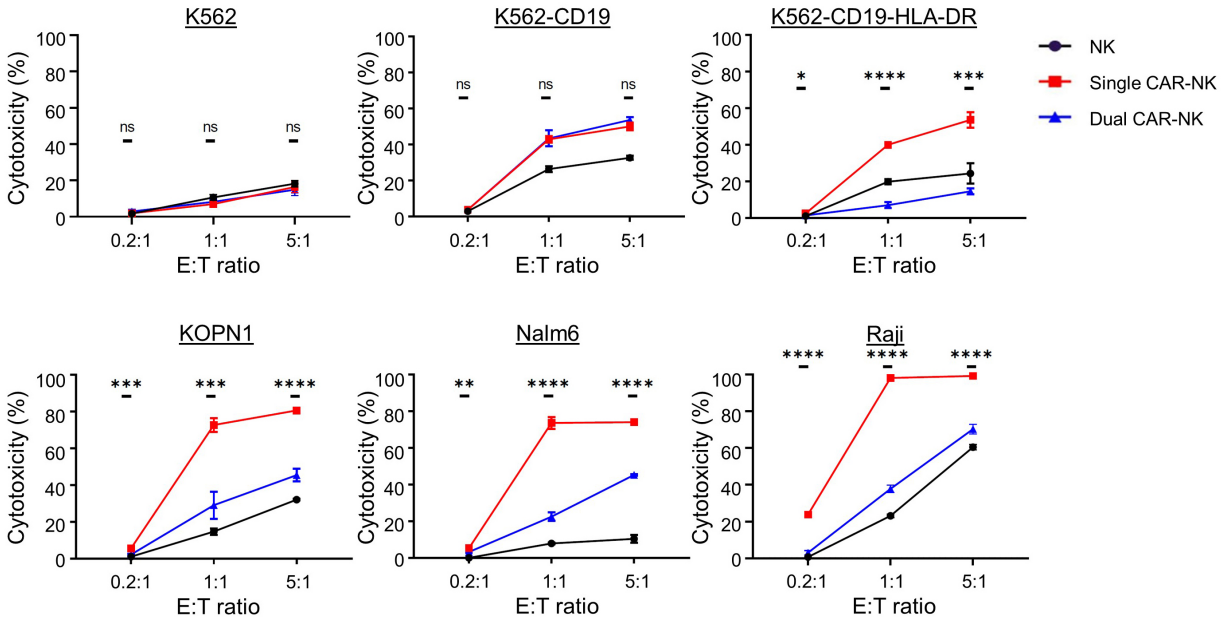

Figure S3. Cytotoxicity of NK and CAR-NK cells against different target cells. NK, single CAR-NK, and dual CAR-NK cells were incubated with K562, K562-CD19, K562-CD19-HLA-DR, KOPN1, Nalm6, or Raji cells at three E:T ratios (0.2:1, 1:1, 5:1) for 4 hours. Cells were then stained with an APC-conjugated anti-CD56 antibody and aqua live/dead stain and subjected to flow cytometric analysis. The percentage of cytotoxicity was calculated as [(A-B)/Ax100], in which A and B were the percentages of viable target cells (CD56-negative) in the control group and the experimental group, respectively. Data are shown as mean ± SEM of three independent experiments. Statistical significance is calculated by unpaired two-tailed Student's t-test. **** p<0.0001; *** p<0.001; ** p<0.01; * p<0.05; ns: not significant.

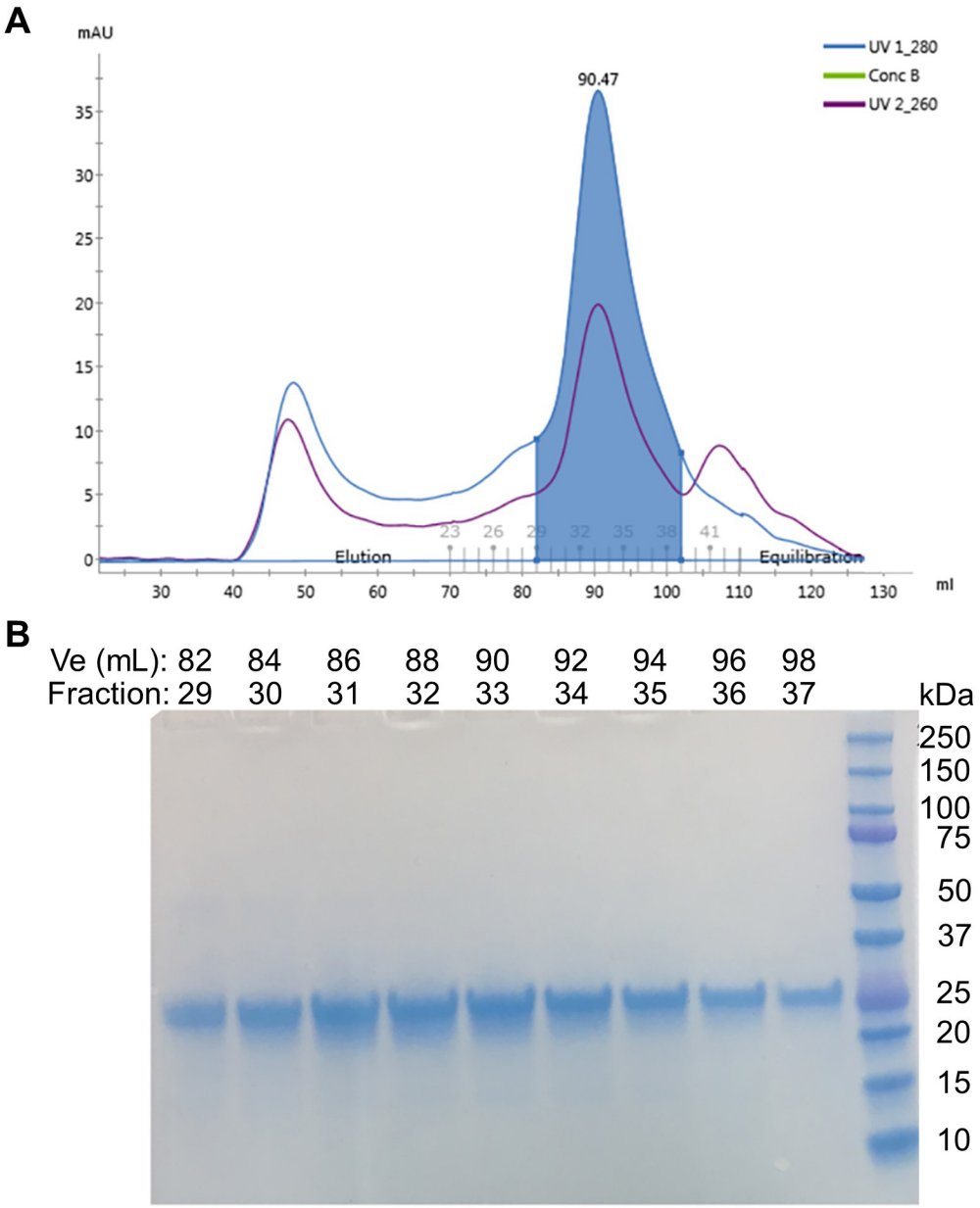

Figure S4. Purification and verification of recombinantly expressed anti-HLA-DR scFv. (**A**) Refolded protein was purified by gel filtration chromatography. The running buffer is 1x PBS buffer pH 7.4. (**B**) Peak fractions were analyzed by SDS-PAGE. Fractions 30-37 were pooled and concentrated to 1 mg/mL for subsequent use.

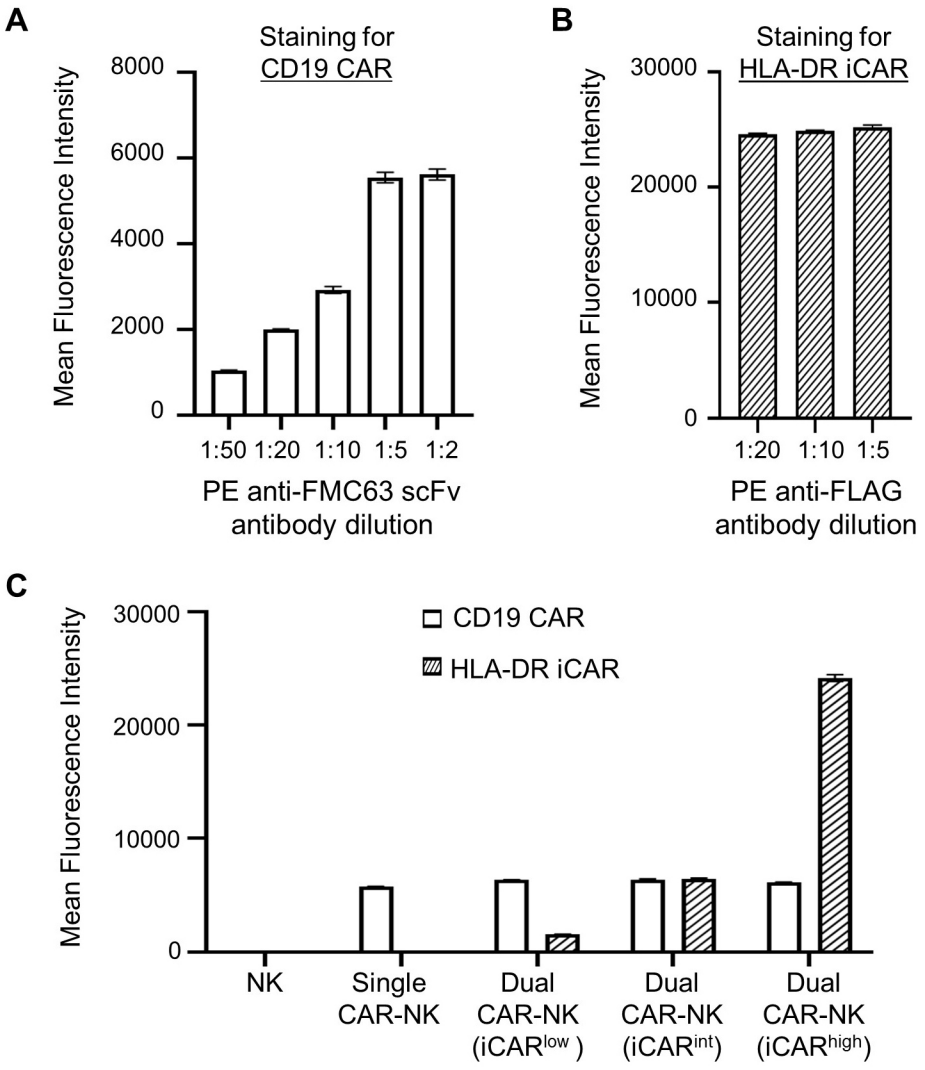

Figure S5. Characterization of dual CAR-NK cells with different levels of iCAR expression. (A)-(B) Titration of the PE-labeled anti-FMC63 scFv antibody (A) and the PE-labeled anti-FLAG antibody (B) for staining the CAR and the iCAR on CAR-NK cells, respectively. Dual CAR-NK ($iCAR^{high}$) cells were stained with each antibody at multiple different dilutions. The mean fluorescence intensities (MFI) of stained cells were measured by flow cytometry. The saturating concentration of each antibody was identified as the minimal concentration at which the MFI of stained cells reached a plateau. **(C)** Comparison of the CAR and iCAR expression on the single CAR-NK cells and three dual CAR-NK cell populations. Cells were stained with the PE-labeled anti-FMC63 scFv antibody at a 1:5 dilution and the PE-labeled anti-FAG antibody at a 1:20 dilution, separately. The MFIs of cells stained with each antibody were measured by flow cytometry. Data were shown as mean ± SEM of three independent experiments.

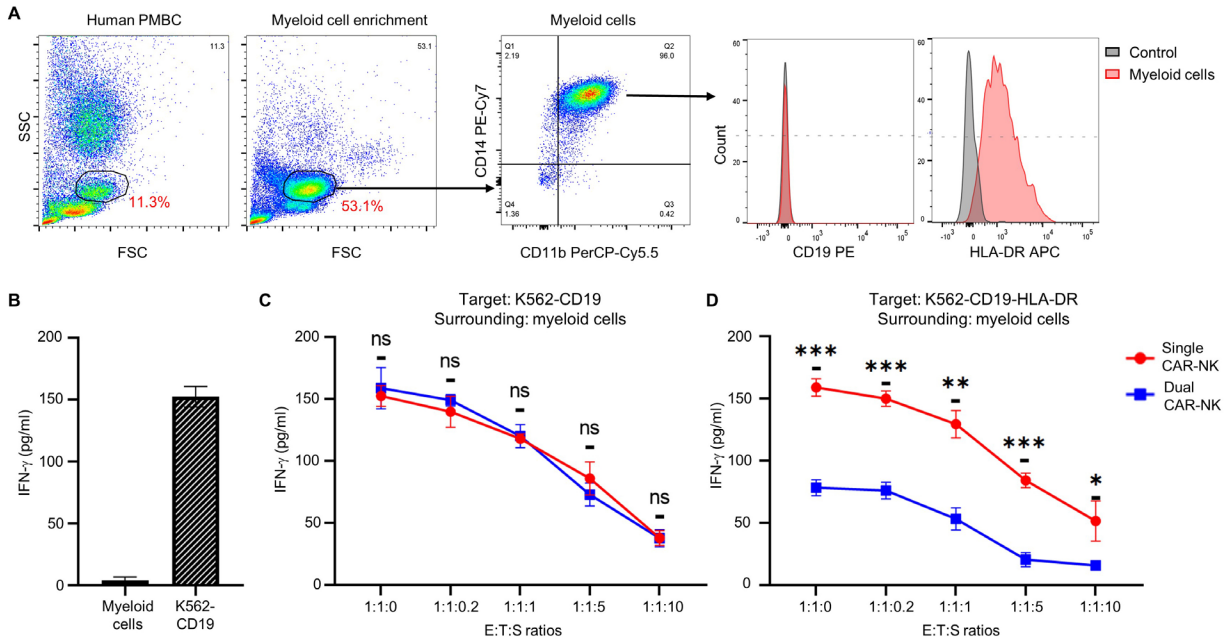

Figure S6. The target selectivity of dual CAR-NK cells is not affected by HLA-DR-expressing surrounding myeloid cells. (A) Myeloid cells in human PBMC were enriched by immunomagnetic negative selection, followed by cell surface marker staining and flow cytometry. The expression or lack of HLA-DR and CD19 was also examined. Isotype antibodies were used as the negative control. Images are representative of three independent experiments with similar results. **(B)** ELISA analysis of IFN-γ production by single CAR-NK cells against myeloid cells or K562-CD19 cells after a 4-hour incubation. Data are shown as mean ± SEM of three independent experiments. **(C)-(D)** Comparison of the activation levels of single and dual CAR-NK cells against K562-CD19 cells (C) or K562-CD19-HLA-DR cells (D) in the presence or absence of human myeloid cells. CAR-NK cells, target cells, and surrounding myeloid cells were cocultured at the indicated E:T:S ratios. After a 4-hour incubation, cell culture supernatants were collected to assess for IFN-γ secretion by ELISA. Data are shown as mean ± SEM of three independent experiments. Statistical significance is calculated by unpaired two-tailed Student's t-test. *** $p<0.001$; ** $p<0.01$; * $p<0.05$; ns: not significant.

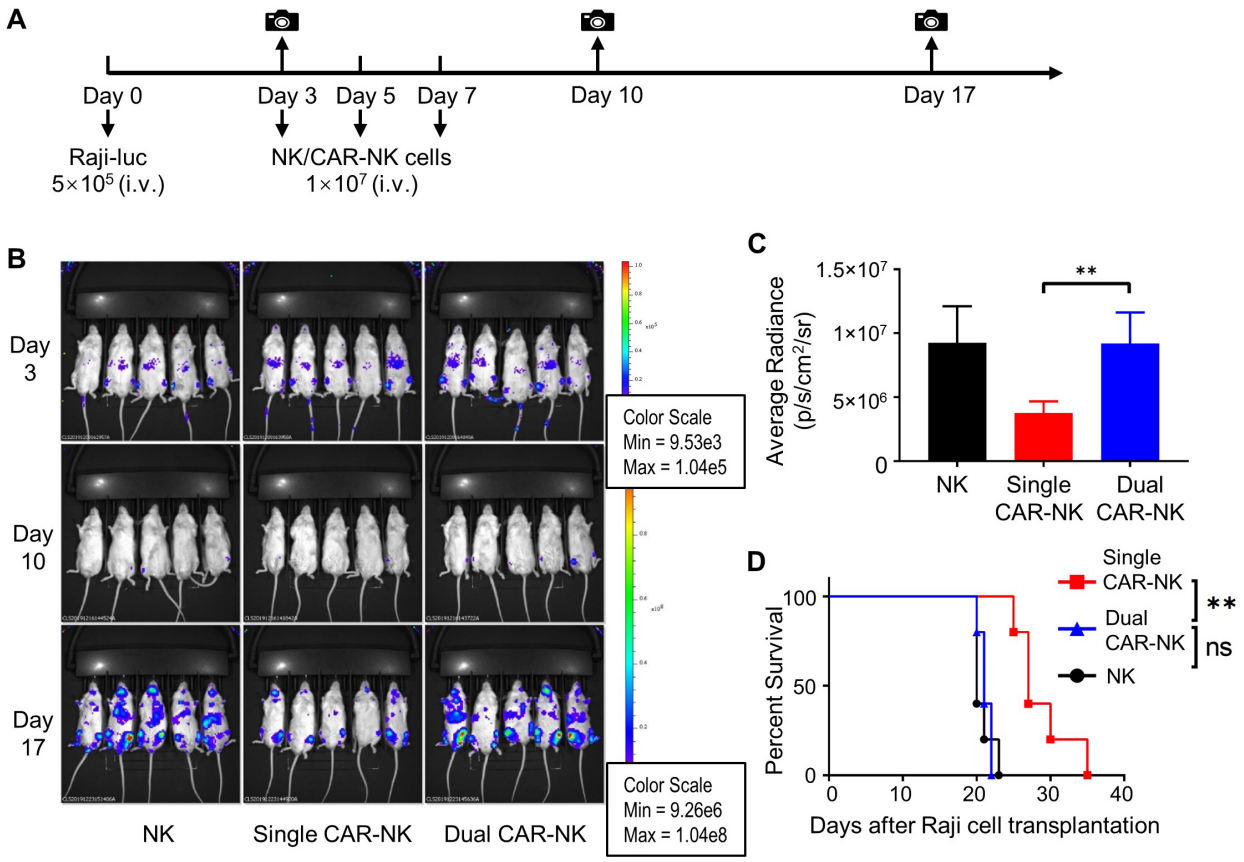

Figure S7. Raji cells ($CD19^+HLA\text{-}DR^+$) are also resistant to dual CAR-NK cell-mediated cytotoxicity *in vivo*. (**A**) Schematic diagram of the *in vivo* killing assay. NSG mice were inoculated with 5×10^5 Raji-Luc cells through tail vein injection on day 0 and then treated with 1×10^7 NK cells, single CAR-NK cells, or dual CAR-NK cells through tail vein injection on days 3, 5, and 7. Tumor growth was monitored by *in vivo* bioluminescence imaging on days 3, 10, and 17. (**B**) Bioluminescence images of tumor growth in mice treated with NK cells (left), single CAR-NK cells (middle), and dual CAR-NK cells (right). (**C**) Quantification of bioluminescence in each treatment group (n=5) on day 17. Data were shown as mean ± SEM. Statistical significance is calculated by unpaired two-tailed Student's t-test. ** $p<0.01$. (**D**) Survival of mice in each treatment group (n = 5) were shown in Kaplan-Meier curves. Statistical significance was calculated by log-rank (Mantel-Cox) test. ** $p<0.01$; ns: not significant.